A computational study of solidification during additive manufacturing of AISI 304 austenitic stainless steel

Conference Paper · December 2019

CITATIONS
2

READS
427

5 authors, including:

Marios P. Sotiriou
University of Thessaly
2 PUBLICATIONS **2** CITATIONS
SEE PROFILE

M. I. T. Tzini
University of Thessaly
14 PUBLICATIONS **24** CITATIONS
SEE PROFILE

John S. Aristeidakis
University of Thessaly
12 PUBLICATIONS **22** CITATIONS
SEE PROFILE

Gregory N Haidemenopoulos
University of Thessaly
158 PUBLICATIONS **2,038** CITATIONS
SEE PROFILE

A computational study of solidification during additive manufacturing of AISI 304 austenitic stainless steel

M.P. Sotiriou[1], M.I.T. Tzini[1], J.S. Aristeidakis[1], G.N. Haidemenopoulos[1,2,3,*], I. Barsoum[2,3]

[1]*Department of Mechanical Engineering, University of Thessaly, Volos, Greece*
[2]*Department of Mechanical Engineering, Khalifa University, Abu Dhabi, UAE*
[3]*Advanced Digital and Additive Manufacturing (ADAM) Research Center, Khalifa University, Abu Dhabi, UAE*
[*]*Correspondence: hgreg@mie.uth.gr*

Abstract

Metallic additive manufacturing (AM) allows production of complex 3D parts directly from CAD models by fusing raw materials with various energy sources. The technology can find wide applications in aeronautics, automotive and chemical industries. Accelerating the adoption of AM requires building on existing knowledge related to energy transfer, non-equilibrium phase transitions and high-performance modeling within an Integrated Computational Materials Engineering (ICME) approach. In this paper a computational study of solidification and associated microsegregation during AM of AISI 304 austenitic stainless steel is presented. The thermodynamics of solidification were investigated, using CALPHAD through the Thermo-Calc software. Thermodynamic and kinetic models of solidification were used, including Scheil-Gulliver and DICTRA simulations, considering diffusion in multi-phase and multicomponent systems. The predicted solidification mode agreed with experimental observations found in the literature. This study enables the identification of suitable models for predicting microstructural evolutions during AM processing of AISI 304 stainless steel.

Keywords: *Additive manufacturing, solidification, 304 stainless steel, microsegregation*

1. Introduction

Additive manufacturing (AM) allows the production of complex three-dimensional parts, impractical or impossible to produce using traditional machining approaches, by fusing a base material via various energy sources. Complex geometry parts produced using AM can yield excellent strength to weight ratios ideal for automotive and aerospace applications. First attempts to develop an object by applying the addition technique were made in 1981 by Hideo Kodama in Japan, regarding polymer materials [1]. The technology expanded to concern metallic materials in the mid 90's. In the following years further research led to upgraded hardware equipment and improvements in both strength and geometrical complexity of the manufactured objects. Despite the extensive research carried out over the years, additive manufacturing remains an open research field, especially in metallic materials, as the number of variables and uncertainties is considerably large.

From the scope of materials science, metallic AM is considered a solidification process where both heat transfer and diffusion occur simultaneously. More specifically, the laser bed fusion process involves rapid heating via laser beam to melt a metallic powder layer, spread over a pre-existing surface using a powder roller or blade. After each laser pass, a new layer of powder is laid and the cycle continuous till the full part emerges. The resulting rapid heating and cooling cycles lead to phase transformations under non-equilibrium conditions [2]. An implication of rapid solidification is the development of elemental microsegregation leading to composition and subsequently physical and mechanical property inhomogeneities. Microsegregation is mainly caused by limited diffusion of substitutional elements in the solid phases, causing compositions to deviate from the nominal, near the solid/liquid interface, as solidification progresses. Thus, fast diffusing elements like carbon usually do not segregate significantly. In non-equilibrium processes, the solidus temperature is affected by the cooling path, since in general, high cooling rates postpone solidification. The low melting regions formed due to microsegregation at the last stages of solidification, can remelt during heat treatment, potentially causing part distortions or other problems in production [2]. Thus, it is important to accurately model solidification related phenomena, in order to predict and avoid microstructures that could impact the performance of a part produced using AM techniques.

The present study constitutes a computational analysis of the solidification mode of the austenitic stainless steel AISI 304 with nominal composition of Fe-18Cr-8Ni-0.08C (in wt %), as a benchmark for

stainless steel and iron-based materials commonly encountered in industry. The study involves AM solidification simulations using different computational thermodynamic and kinetic models based on CALPHAD. The aim of this study was to determine a suitable simulation model for the AM process, as well as gain insight over the phenomena controlling the microstructure evolution. Specific AM process parameters were quantified and model predictions were compared to experimental data from the literature [3-5].

2. Methodology

The objective of the present study was to simulate the metallurgical phenomena taking place during the AM process and mainly the solidification process, using computational thermodynamics and kinetics based on the CALPHAD approach. The plethora of phenomena involved during solidification add to its complexity. Several simulation models were employed, each based on a different set of assumptions and approaching the phenomenon from a slightly different angle. The validity of the model assumptions where examined and simulation results where compared to determine which model better describes solidification under additive manufacturing conditions. Initially the limiting case of equilibrium solidification is investigated, which, despite being not applicable for AM conditions, provides useful information regarding the system's thermodynamic properties. Next the effect of the cooling rate was investigated during solidification under non-equilibrium conditions, initially assuming an infinitely high value with the Scheil-Gulliver approach and then simulating a finite value with the DICTRA model, better approximating the conditions during AM.

2.1 Equilibrium Solidification

The required thermodynamic calculations were performed, using thermodynamic databases, in the Thermo-Calc software, which is based on the CALPHAD approach to describe the Gibbs free energy of each phase in the system. The database in use, was the TCFE6, containing thermodynamic information addressed to ferrous alloys. Thermodynamic analysis of stainless steels stated the importance of a linear structure, the tie triangle (depicted as the ABC triangle in Figure 2a, contained in the Cr and Ni-isopleth diagrams, existing in the border with the liquid area. The solidification's type can be characterized based on which vertical path relative to the corners of the triangle, the solidification path proceeds. Furthermore, the major phases are the FCC matrix phase (γ-Fe), the BCC matrix phase (δ-Fe) and the Liquid.

In the present work, thermodynamic calculations were performed first at equilibrium conditions, in order to provide information about solidification under near equilibrium conditions. The solidification path through the isopleth sections of the phase diagrams, assumes infinitesimal cooling rate so that transformations take place under equilibrium conditions. The simulation described above is named Equilibrium Solidification and outlines the limiting event of having a cooling rate of infinitely small value, a fact that diverges the simulation from the AM conditions, yet providing useful information regarding the behavior of the system.

2.2 Non-equilibrium Solidification: The Scheil-Gulliver approach

During AM processes, the laser beam develops high temperatures at the point of impact, forcing the raw material (e.g. powder) to melt. As the beam travels to other areas, the material solidifies under high cooling rate and therefore non-equilibrium conditions. Based on the magnitude of the cooling rate values, the Scheil-Gulliver model attempts to simulate the solidification procedure. Scheil-Gulliver's basic assumptions are the homogenization of the liquid phase (considering infinite diffusion), the prevention of solid-state diffusion, during or after the solidification (simulation of infinite values of the cooling rate) and local equilibrium at the solid/liquid interface. Two different simulations were performed based on the Scheil-Gulliver approach, with the difference being to allow or suspend the transformation of the BCC (δ-Fe) phase to the FCC (γ-Fe) phase. Both cases were taken into account in order to allow model comparison. The phenomenon of microsegregation was observed and quantified in both cases. Finally, in order to ensure computational stability, the simulation terminated at 98% of the solidification process.

2.3 Non-equilibrium Solidification: DICTRA Solidification

Considering the kinetics of solidification upon cooling, with a finite cooling rate, requires the solution of diffusion equations in a multi-component, multi-phase system with moving boundaries. Kinetic simulations were performed using the DICTRA module of Thermo-Calc, with the MOBFE2 mobility and TCFE6 thermodynamic database. The kinetic problem was considered in a one-dimensional, planar geometry diffusion cell, with a size of 100μm, representative of the as solidified microstructure, according to the literature. Furthermore, the cell constitutes a closed thermodynamic system. In the present work a cooling rate of 1°C/s was assumed, starting from a temperature of 1500°C and ending the simulation at 1300°C, based on thermodynamic data.

Thermodynamics suggest that only three phases participate in the solidification process, Liquid, BCC and FCC. There are two possible modes of solidification depending on various conditions, eutectic and peritectic solidification. To simulate eutectic solidification the FCC/Liquid/BCC model was used, from now on referred as FLB. In this case the diffusion cell is composed of a region of FCC, a region of BCC and a liquid region in-between, as shown in Figure 1a. During cooling BCC and FCC nucleate accordingly and grow against the liquid. Peritectic solidification is modeled using the Liquid/FCC/BCC (LFB) model, as shown in Figure 1b. In this case, as temperature decreases BCC nucleates and grows against the liquid and at a critical temperature, FCC nucleates and grows against both other phases. Similar to the Scheil-Gulliver approach, both simulations were performed and their characteristics were quantified for model comparison and to select the most suitable model able to describe the microstructure evolution during solidification.

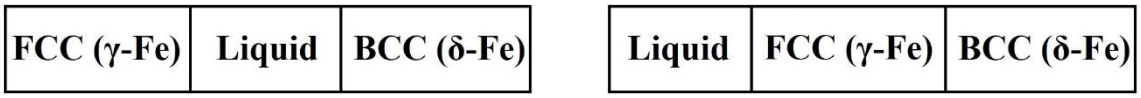

(a) **(b)**

Figure 1. Representation of DICTRA (a) FLB and (b) LFB calculation cell.

3. Results and discussion

3.1 Equilibrium calculations

In multicomponent systems, isopleth sections of the phase diagram are very useful for the study of phase transformations. Figure 2a depicts the Cr whereas Figure 2b the Ni isopleth section of the AISI 304 alloy, by setting all compositions equal to the nominal and allowing only the element of interest to vary on the x-axis.

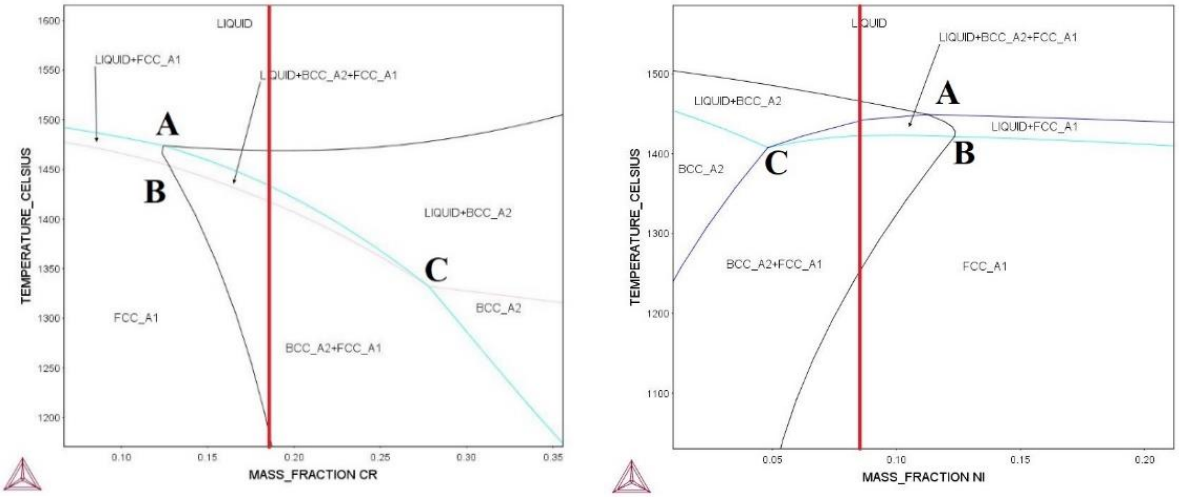

(a) **(b)**

Figure 2. Phase diagram sections (isopleths) for (a) constant C and Ni and (b) constant C and Cr for the Fe-18Cr-8Ni-0.08C wt % stainless steel.

In both figures the tie triangle (named ABC) is visible, while the vertical lines represent the solidification path of the subject steel, when performed under equilibrium conditions. As observed in isopleths, the solidification path for the 304SS, first crosses the liquidus line, entering in L + BCC (δ-

Fe) region, where BCC begins to grow. As solidification progresses, the AC side of the tie triangle is crossed, characterizing the solidification as type FA or Ferritic-Austenitic, meaning that during the solidification process, ferrite forms prior to austenite. Moreover, in an FA type solidification the microstructure is either lacy (alternating lamellas of ferrite/austenite) or vermicular (skeletal ferrite), depending on whether eutectic or peritectic solidification takes place. The solidification ends when the path crosses the BC solvus line, entering a two-phase region of FCC (γ-Fe) + BCC (δ-Fe). The freezing range, defined as the difference between liquidus and solidus, appears to have a value of 50°C. Furthermore, comparing the above calculations to a ternary Fe-18Cr-8Ni (wt %) system, revealed that a minor variation in carbon composition is able to alter the solidification type from FA to F, where only ferrite is nucleated from the liquid. The equilibrium solidification model predicts a volume fraction of 70% BCC and 30% FCC, while there is no microsegregation at the end of solidification.

3.2 Scheil-Gulliver Calculations

Two different simulations were performed based on the Scheil-Gulliver approach, one with allowing and the other with suspending the BCC to FCC transformation during the simulation. The simulation that allows the transformation is referred as Y and the one that suspends it, as N simulation. In Figures 3a and 3b, the Cr and the Ni content of each phase are ploted versus the fraction of solid during solidification accordingly, only for the Y simulation, though results for the N case are similar. The minimum and maximum elements concentrations due to microsegregation are presented (in wt %) in Table 1. It is observed that the liquid becomes enriched in alloying elements, requiring additional cooling to solidify and solid phases develop elemental segregation at late solidification stages, as shown in Figure 3 for the Y case. The fraction of solid vs temperature and the volume fraction of δ-ferrite (BCC) vs temperature are depicted in Figure 4a and 4b respectively. The Y simulation displays a freezing range of 63°C, while the N simulation displays an increased value of 103°C. Note that both simulations exhibit a wider freezing range compared to equilibrium. Allowing the BCC (δ-Fe) to FCC (γ-Fe) transformation, simulates peritectic solidification and by suspending it, simulates eutectic solidification, explaining the temperature difference in the freezing range predicted by the two models. The reason behind the deviation from equilibrium, is that Scheil models solidification under rapid cooling, where diffusion is negligible in the solid phases and each phase solidifies with the instantaneous composition of the liquid. In Figure 4b, Scheil-Gulliver model tend to develop a BCC fraction around 75% for both simulations.

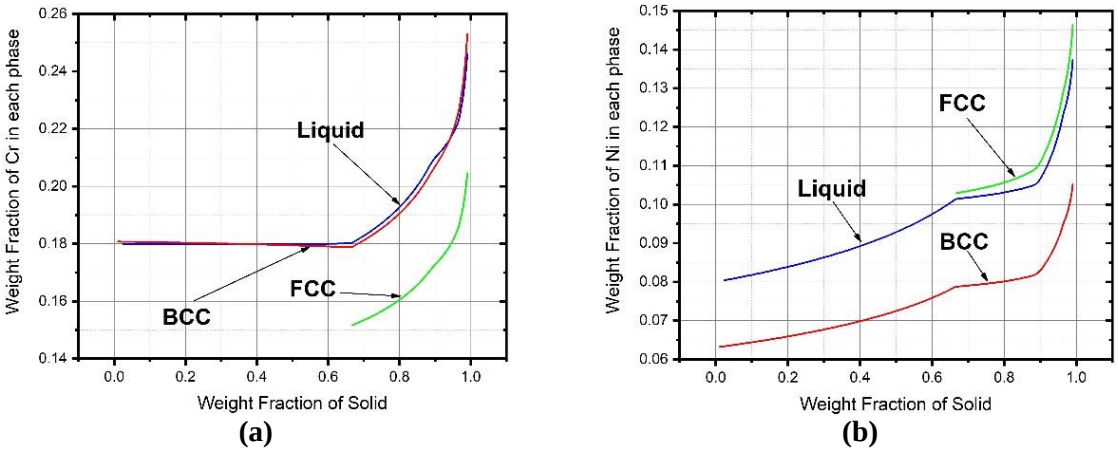

(a) **(b)**

Figure 3. Microsegregation of (a) Cr and (b) Ni in all phases, predicted by Scheil Y simulations.

Table 1. Minimum and maximum concentration (wt%) of elements in each phase due to microsegregation according to the Y Scheil-Gulliver simulation.

	C		Cr		Ni	
	Minimum	Maximum	Minimum	Maximum	Minimum	Maximum
BCC	0.01%	0.02%	17.9%	25.3%	6.3%	10.5%
FCC	0.06%	0.08%	15.2%	20.5%	10.3%	14.6%

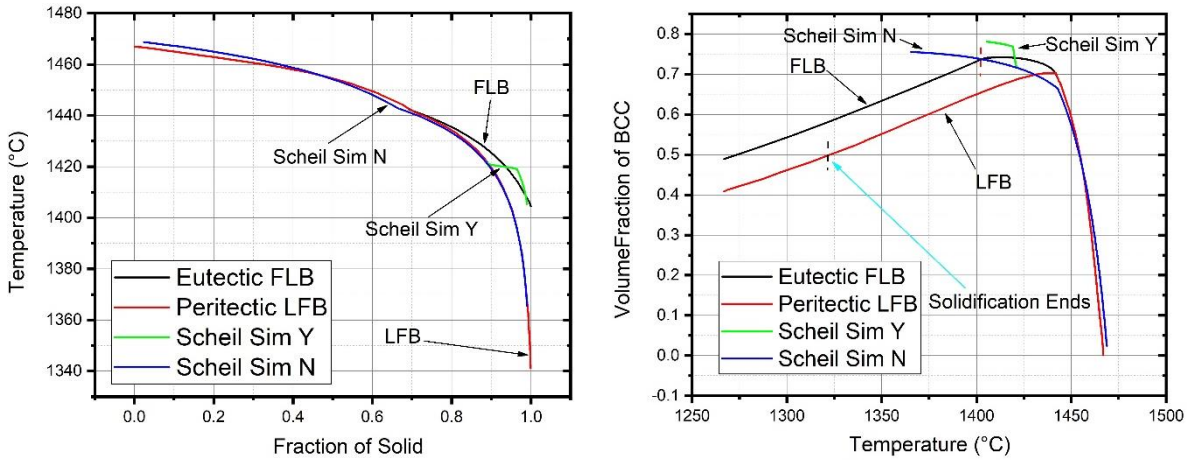

(a) **(b)**

Figure 4. Model comparison of the predicted (a) Solidification paths and (b) BCC (δ-Fe) phase fraction.

3.3 DICTRA calculations and model comparison

Regarding DICTRA simulation results, the FLB (FCC/Liq/BCC) simulation, displayed a freezing range of 63°C, similar to the Scheil Y simulation and the LFB (Liq/FCC/BCC) model, displayed 125°C, the highest value encountered in the study, as indicated in Figure 4a**.** This is due to sluggish diffusion of substitutional elements like Cr & Ni, in the solid phases, making solid state diffusion the controlling factor for solidification. In Figure 4b, the volume fraction of BCC developed in the FLB simulation reaches a value around 74%, while the peritectic LFB reaches a value of only 49%. Composition profiles as a function of distance in the diffusion cell, at various time intervals are presented in Figure 5, for the FLB model. The vertical lines represent the position of the interface of two neighboring regions. Initially only the liquid phase is present. As temperature decreases with a rate of 1°C/s, BCC nucleates and grows against the liquid. At a critical temperature FCC nucleates and both BCC and FCC grow against the liquid as eutectic solidification proceeds. Due to sluggish diffusion, liquid becomes enriched in Cr and Ni. After solidification, microsegregation is observed in both solid phases, as FCC has less Cr and more Ni compared to the equilibrium, whereas BCC exhibits the opposite behavior.

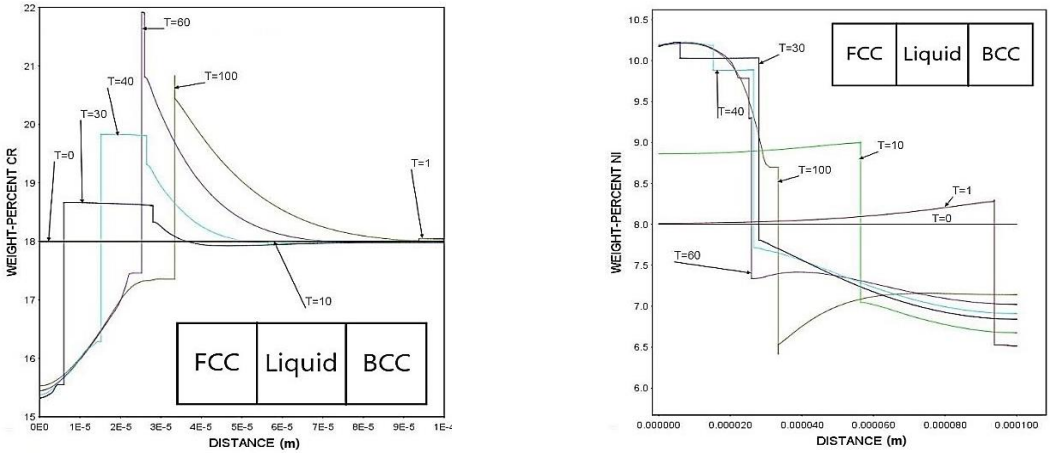

(a) **(b)**

Figure 5. Eutectic FLB simulation concentration profiles for (a) Cr and (b) Ni, at t=1, 10, 30, 40, 60, 100s. Segregation is present at the end of solidification.

Composition profiles for the LFB case are presented in Figure 6. Starting from liquid, BCC nucleates and grows as in the FLB model. However, FCC nucleates on the liquid/BCC interface and grows against both, as peritectic solidification proceeds, until all liquid is consumed. Segregation profiles are similar to those of the FLB model, with the exception that Cr rises rapidly while Ni drops in the FCC, at late stages of solidification. The process is limited by the diffusion of substitutional elements and thus the

freezing range is extended, resulting in the formation of intense segregation profiles. Note that C does not form a segregation profile in both cases, since it is a fast diffusing element.

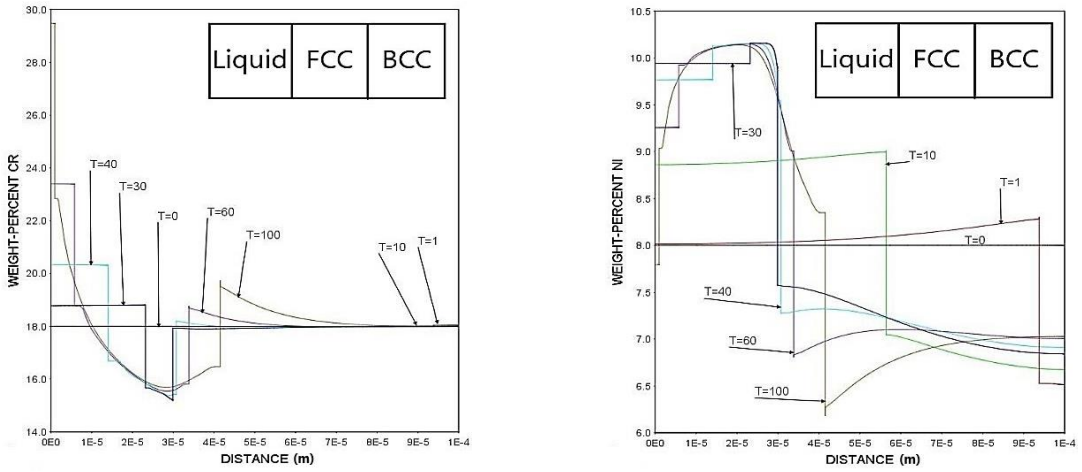

(a) **(b)**

Figure 6. Peritectic LFB simulation concentration profiles for (a) Cr and (b) Ni, at t=1, 10, 30, 40, 60, 100s. Segregation is present at the end of solidification.

The comparison of the simulation models revealed an agreement among the solidification paths of Scheil-Gulliver and DICTRA simulations. More specifically, the Scheil-Gulliver Y simulation resembles the DICTRA FLB simulation since both model a eutectic reaction while the Scheil-Gulliver N simulation resembles the DICTRA LBF simulation, modelling a peritectic reaction. Although solidification paths match, the final phase constitution is not analogous. While both Scheil-Gulliver simulations tend to agree with the FLB simulation with respect to the formed BCC volume fraction, the peritectic LFB resulted to the lowest BCC fraction. This seems to be an effect caused by slow diffusion in the (γ-Fe) region. Experimental evidence [3-5] focused on the temperature and freezing ranges, indicated that for the AISI 304 steel, the DICTRA peritectic LFB simulation best described the observed microstructures, though Scheil simulations that allowed the BCC to FCC transformation were also close.

4. Conclusions

The solidification of an AISI 304 stainless steel was investigated using computational thermodynamic and kinetic modelling in the form of Scheil-Gulliver and DICTRA simulations. Two different simulation models were considered, corresponding to eutectic and peritectic solidification. Each model was based on different assumptions regarding the diffusion kinetics. A general agreement between Scheil-Gulliver (Y/N) and DICTRA (FLB/LFB) simulation results was observed. The diffusion of substitutional elements (Cr&Ni), influences the freezing range and the solidification path. DICTRA simulations using the peritectic LFB model, resulted to the highest freezing range and the smallest BCC fraction, with good agreement with experimental observations obtained from literature.

References

1. Kodama, H. (1981). A scheme for three-dimensional display by automatic fabrication of three-dimensional model. *IEICE Trans. on Electronics*, 237-241.
2. Haidemenopoulos, Greg. (2018). *Physical Metallurgy*. Boca Raton: Taylor and Francis.
3. Fu, J. W., & Yang, Y. S. (2013). Origin of the lathy ferrite in AISI 304 stainless steel during directional solidification. *Journal of Alloys and Compounds*, *580*, 191-194.
4. Ma, J. C., Yang, Y. S., Tong, W. H., Fang, Y., Yu, Y., & Hu, Z. Q. (2007). Microstructural evolution in AISI 304 stainless steel during directional solidification and subsequent solid-state transformation. *Materials Science and Engineering: A*, *444*(1-2), 64-68.
5. Saied, M. (2016). *Experimental and numerical modeling of the dissolution of delta ferrite in the Fe-Cr-Ni system: application to the austenitic stainless steels* (Doctoral dissertation, Grenoble Alpes).